

## ANALYSIS OF DROUGHT INDICES IN THE UPPER LUK ULO WATERSHED, CENTRAL JAVA, INDONESIA

MUHAMMAD FARHAN ATHAYA AND SLAMET SUPRAYOGI\*

Department of Environmental Geography, Faculty of Geography, Universitas Gadjah Mada, Sekip Utara, Bulaksumur,  
55281 Yogyakarta, Indonesia.

\*Corresponding author: [ssuprayogi@ugm.ac.id](mailto:ssuprayogi@ugm.ac.id)

<http://doi.org/10.46754/jssm.2025.09.007>

Submitted: 14 September 2023 Revised: 9 January 2025 Accepted: 3 March 2025 Published: 15 September 2025

**Abstract:** This study assesses drought in the upper Luk Ulo Watershed, a repeatedly affected area in Central Java, Indonesia. The Thornthwaite water balance was utilised to calculate water availability, Palmer Hydrological Drought Index (PHDI) and Palmer Drought Severity Index (PDSI) were employed to determine drought conditions. Both analyses were based on the locations of three rain gauge stations: Wadaslintang, Karangsambung, and Singomerto. Using 10 years of rainfall data (2011–2020), the highest water availability in the proximal areas of the three stations occurred in 2016. In the same year, PHDI and PDSI values indicated severe wet and extremely wet spells, respectively. In contrast, the lowest water availability was recorded in 2019 in Wadaslintang and Karangsambung, 2015 in Singomerto. PHDI identified the most severe drought (incipient dry spell) in 2014 in Karangsambung and Singomerto, causing the most extensive impact, affecting an area of 257.38 km<sup>2</sup>. Meanwhile, PDSI showed the most severe and extensive drought (incipient dry spells) in 2019 and 2020 in Karangsambung and Wadaslintang, affecting an area of 202.14 km<sup>2</sup>. Based on the number of spells, PHDI and PDSI classified the majority of the conditions as dry, but none were identified as extremely dry.

Keywords: Water balance, water availability, drought indices, Palmer Hydrological Drought Index (PHDI), Palmer Drought Severity Index (PDSI).

### Introduction

Water is an essential resource for sustaining human life and other living organisms that consequently requires proper management to ensure environmental sustainability. When available, water fulfills humans' daily drinking needs that are substantial for their metabolism and health, support domestic and industrial activities. It is also needed by animals and plants to preserve biodiversity and food security. Calculating water balance is one of the approaches to ensure water availability. Water balance explains that the inflows to a certain place in any period are equal to or form a balance with the outflows, which is related to the changes in water and energy at the Earth's surface (Gao *et al.*, 2010; Thompson, 2017; Asriningrum *et al.*, 2019). Here, water availability is conceptually described as surplus or deficit depending on the difference between the input and output that makes up changes in water storage, which is a determinant of drought occurrence. As a

natural disaster, drought negatively affects the environment and its dependents. For instance, low water availability can lead to crop failure and even human fatalities (Hidayati & Suryanto, 2015; Mediani *et al.*, 2019). Moreover, since food production heavily relies on water availability, water crises pose a major threat to food security (Sanim, 2018).

In water balance, drought is a hydrometeorological phenomenon indicated by an abnormal and prolonged water deficit (American Meteorological Society, 2019). It, however, does not necessarily turn into a disaster unless a direct adverse impact is felt in the social, economic, and environmental aspects of people's lives (Aryo & Lubis, 2014). Drought is categorised as a slow-onset disaster as it appears gradually and slowly due to interactions between various events (United Nations Office for the Coordination of Humanitarian Affairs, 2011). The onset of drought is difficult to determine

and predict, its impact may be felt differently in each region (Funk & Shukla, 2020).

There are four type of droughts: Meteorological, hydrological, agricultural, and socioeconomic. Meteorological drought refers to long-lasting rainfall deficits while hydrological drought occurs due to meteorological drought that affects the availability of water in rivers, reservoirs, and groundwater systems (Dey & Lewis, 2021; Faiz *et al.*, 2022). When the soil’s moisture content decreases below the minimum amount required for plant growth, this condition is called agricultural drought. It can lead to crop failure and low agricultural yields, thus, impacting agricultural loss (Dalezios *et al.*, 2017; Faiz *et al.*, 2020). Socio-economic drought is a situation where the available water demand cannot meet the water needs of multiple sectors, including agriculture, resulting in economic losses (Liu *et al.*, 2020; Faiz *et al.*, 2020; Faiz *et al.*, 2022). Factors contributing to drought

include low rain, increased air temperature, and low humidity (Sen, 2015).

Drought severity is characterised according to duration, intensity, spatial coverage, and the diversity of environmental features and economic activities in the affected area (Shaw *et al.*, 2010). For this reason, composite indices are used to detect and monitor drought as they can classify it into degrees of severity from the driest to the wettest, provide information on its temporal variations. Table 1 describes several types of commonly used drought indices and their limitations.

Drought monitoring is crucial to understand the time and length of a drought event and detect its occurrence to mitigate the negative environmental and societal impacts. A drought index quantifies drought severity using multiple indicators in a particular area and time (World Meteorological Organisation & Global Water Partnership, 2016). It provides a streamlined

Table 1: Comparison of several drought indices

Drought Indices	Description	Limitations
Standardised Precipitation Index (SPI)	Standardises precipitation to compare different regions and timescales in terms of their precipitation anomalies. Can be used to reflect meteorological drought. Its simplicity can describe wet and dry period based on precipitation data only (Cheval, 2015)	<ul style="list-style-type: none"> <li>• Does not differentiate a region’s proneness to drought and does not consider the pre-drought moisture condition (Cheval, 2015)</li> <li>• Does not consider the effect of temperature on droughts (Faiz <i>et al.</i>, 2022)</li> </ul>
Standardised Precipitation Evapotranspiration Index (SPEI)	A developed version of SPI with potential evapotranspiration derived from air temperature considered as one of drought driving factors (Lee <i>et al.</i> , 2024)	<ul style="list-style-type: none"> <li>• The unavailability of air temperature data in certain areas can hinder the calculation process (Tefera <i>et al.</i>, 2019)</li> </ul>
Palmer Drought Indices: Palmer Hydrological Drought Index (PHDI) and Palmer Drought Severity Index (PDSI)	PHDI describes the condition of hydrological drought, while PDSI refers to meteorological drought. Both are calculated based on water balance supply and demand concept (Palmer, 1965). Both indices also consider normal condition through climatically appropriate for existing conditions (CAFEC) calculation, which is based on climate characteristics of each region	<ul style="list-style-type: none"> <li>• These indices were designed for long-term drought monitoring (monthly) and may not respond effectively to short-term or rapidly changing drought conditions (Eslamian <i>et al.</i>, 2017)</li> <li>• The 1-monthly analysis of the indices may be difficult to correlate with other hydrological variables (Dai &amp; NCAR, 2023)</li> </ul>

way to describe, understand, and compare complex drought events. One such index is the Palmer drought index, which incorporates water balance components and the concept of climatically appropriate for existing conditions (CAFEC). CAFEC is derived from coefficients of evapotranspiration, soil moisture recharge, soil moisture loss, and runoff to determine water loss according to existing climate conditions (Kurniawan *et al.*, 2020). This calculation produces the CAFEC coefficient, i.e., the ratio of the average occurrence of a parameter to its potential value (Palmer, 1965), thus, providing information on what constitutes the normal conditions of water supply and demand in an area (Weber & Nkemdirim, 1998).

In water balance, precipitation and moisture loss are the inflows (supply) to the watershed system while evapotranspiration, runoff, and moisture recharge are the outflows (demand). CAFEC distinguishes between dry conditions caused by an average dry season and an abnormally dry period. This also applies to wet conditions. This differentiating ability of CAFEC corresponds to Palmer's definition of drought (1965), i.e., an abnormal moisture deficit. Identifying normal conditions before calculating the index is necessary to determine abnormality (Weber & Nkemdirim, 1998).

The Palmer drought index comprise the Z index, Palmer Hydrological Drought Index (PHDI), and Palmer Drought Severity Index (PDSI). The Z index shows moisture anomaly to determine the beginning and end of a dry or wet spell, it offers an empirical approach to determine the drought index (Yan *et al.*, 2013). With a known Z index, two components of the Palmer drought index, PHDI and PDSI can be calculated. The fundamental difference between the two is that PHDI describes the conditions of a hydrological drought while PDSI refers to a meteorological drought. As a result, both use different concepts to determine the end of a dry or wet spell. In PHDI, the spell change is observed in the last month where the water supply and demand return to normal, whereas in PDSI, it is determined in the first month of

a sequence of months where the weather starts to change to near normal, as indicated by the probability of the spell's ending (Karl *et al.*, 1987).

Drought has been reported in numerous areas in Indonesia, including Kebumen in Central Java. According to the Government of Kebumen Regency (2015), there has been widespread, recurrent drought in the mountainous areas. The Luk Ulo River flows through Kebumen, originating in the South Serayu Mountains (part of the Karangsambung-Karangbolong National Geopark) and emptying into the Indian Ocean in the south. Saifudin and Raharjo (2008) stated that the river does not dry up but still flows during the dry season, although at a severe low discharge.

The Luk Ulo watershed administratively lies in three regencies: Kebumen, Banjarnegara, and Wonosobo. Districts in Kebumen that belong to the Karangsambung-Karangbolong National Geopark are Karangsambung, Karanggayam, Ayah, Buayan, Adimulyo, and Ambal, with the first two districts having the highest susceptibility to drought based on low groundwater quantity due to local geological conditions and a history of drought occurrences (Saputro & Mulyasari, 2019). Land conversion and sand mining in the upper Luk Ulo watershed have led to land degradation (Raharjo, 2009). Sand mining is known to reduce water levels in public and residential wells, as it reduces ground water recharge, resulting in water scarcity (Arsal *et al.*, 2016).

Drought can cause a variety of problems, both environmentally, socially, and economically. Thus, the problems caused by drought can affect the food security and water resources of a community and it is important to understand its onset, duration, and severity (Faiz *et al.*, 2020). Therefore, to further understand the characteristics of drought in the upper Luk Ulo watershed, a drought indices study was conducted based on water balance parameters involving hydrometeorological and physiographic data of the watershed.

The objectives of this study are to (1) analyse water availability in the upper Luk Ulo watershed and (2) analyse the PHDI and PDSI in the upper Luk Ulo watershed. Water availability is represented using the Thornthwaite water balance concept, which provides the foundational data for calculating the Palmer drought indices. The indices were selected for their ability to examine long-term drought conditions, as the area is frequently affected by drought. Moreover, by accounting for both atmospheric and terrestrial factors, the indices offer a more comprehensive reflection of the water balance compared with other drought indices.

### Research Location

The upper Luk Ulo Watershed spans parts of the Kebumen, Banjarnegara, and Wonosobo Regencies (Figure 1). It was elected for this study due to its function in capturing, collecting, and channelling rainwater to the middle and lower watersheds, which cover the majority of Kebumen Regency. The degraded condition of the upper watershed is a concern, as it may negatively impact downstream areas. Saputro and Mulyasari (2019) discovered high levels

of drought hazards in Karangsembung and Karanggayam, both located within the upper watershed. Additionally, the local government identified widespread drought across 94 districts and the mountainous regions.

Furthermore, drought occurrences in the upper and entire Luk Ulo Watershed remain underexamined. While there have been several drought studies in and around the research location, the analyses centred on administrative units, not on the watershed scale. Therefore, focusing on a watershed system as the research object is expected to represent the entire hydrological system that controls the processes leading to a drought event.

### Research Methods

#### Data

The study utilised primary and secondary data. The primary data consisted of soil texture information, derived from sampling in the field and subsequent laboratory analysis. Soil samples were collected based on the landform map, with sampling points determined for each landform type. Secondary data included rainfall, temperature, land use/land cover, and digital elevation model (Table 2).

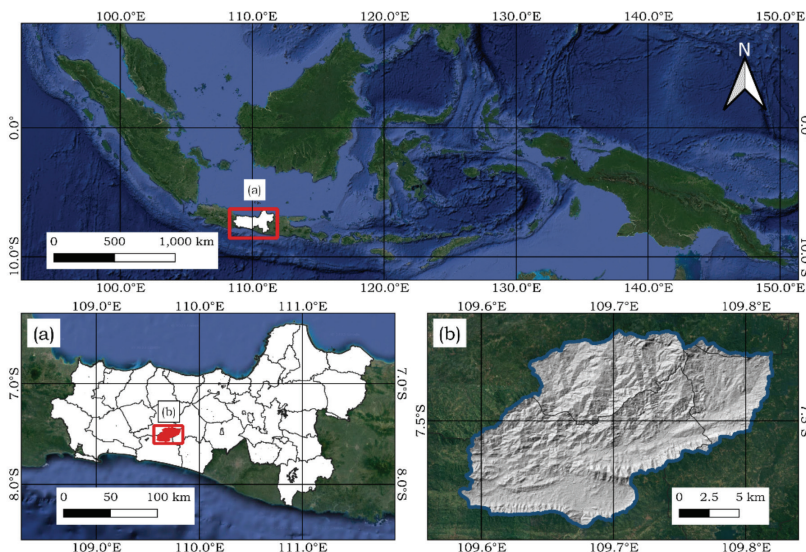


Figure 1: Map of the study area: (a) Central Java Province on Java Island, Indonesia and (b) Upper Luk Ulo Watershed

Table 2: Research data source and usage in the analysis

No.	Data	Data Source	Data Usage
1.	Soil texture	Rapid screening and laboratory analysis	To calculate available water capacity
2.	Rainfall	Serayu-Opak River Region Centre (BBWS)	To calculate water balance and drought indices
3.	Temperature	Serayu-Opak River Region Centre (BBWS)	To calculate evapotranspiration
4.	Land use	Geoportal of Central Java Province	To calculate water holding capacity
5.	Digital Elevation Model (DEM)	Geospatial Information Agency (BIG)	To delineate watershed and produce a landform map

**Water Availability Analysis**

Water availability is a function of rainfall, temperature, evapotranspiration, and soil moisture. For the upper Luk Ulo Watershed, rain data from three stations were mapped to obtain and visualise the regional rainfall. This mapping aimed to determine the area of influence or the proximal area of each station to calculate the spatial average of the rainfall data so that this area can be used for analysis. This process employed the Thiessen polygon method, which involves forming triangles from neighbouring stations and drawing perpendicular bisectors to each side of the triangle.

The air temperature at each rainfall station was determined from temperatures at the nearest climatology stations with the most complete data. It was then calculated by utilising the elevation difference between the two stations, as written in the Mock formula below:

$$\Delta t = Z_1 - Z_2 \times 0.006 \tag{1}$$

$$t_2 = t_1 + \Delta t \tag{2}$$

where  $\Delta t$  is the temperature difference between the watershed and the climatology station ( $^{\circ}\text{C}$ ),  $t_2$  is the watershed's temperature ( $^{\circ}\text{C}$ ),  $t_1$  is the temperature at the climatology station ( $^{\circ}\text{C}$ ),  $Z_1$  is the elevation of the climatology station (m), and  $Z_2$  is the elevation of the rainfall station (m).

Potential evapotranspiration ( $PET$ ) was expressed in cm/month and calculated using the Thornthwaite equation:

$$PE = PET \left[ \frac{s.TZ}{30 \times 12} \right] \times 10 \tag{3}$$

$$PET = 1.6 \left[ \frac{10 \times t}{I} \right]^a \tag{4}$$

where  $PE$  is the corrected potential evapotranspiration (mm/month),  $(s.TZ/30 \times 12)$  is a correction factor for the duration of sunlight that varies with latitude, and  $t$  is the average monthly temperature ( $^{\circ}\text{C}$ ). The yearly heat index  $I$  and the place coefficient  $a$  were:

$$I = \left( \frac{t}{5} \right)^{1.514} \tag{5}$$

$$a = (675 \times 10^{-9} \times I^3) - (771 \times 10^{-7} \times I^2) + (1792 \times 10^{-5} \times I) + 0.49239 \tag{6}$$

Water surplus or deficit was determined using the Thornthwaite water balance by calculating the components below:

(1) Accumulated Potential Water Loss (APWL) was calculated based on the difference between rainfall and potential evapotranspiration, with the provisions explained below:

- If  $P > PE$ ,  $APWL = 0$ .
- If  $P < PE$ ,  $APWL =$  the cumulative sum of the absolute  $P-PE$  in each month and the previous month.

(2) Available Water Capacity (AWC) or soil moisture capacity was calculated by overlaying the land use map with the soil

texture map and multiplying available water, root thickness, and area. The available water was estimated from the soil texture in each proximal area of the rainfall station (Thiessen polygon). Soil texture data were obtained from purposive sampling at locations selected to represent all landforms in the watershed while considering accessibility (Figure 2).

(3) Soil moisture storage ( $St$ ) was determined based on the Accumulated Potential Water Loss (APWL):

- If  $APWL = 0$ ,  $St = AWC$
- If  $APWL \neq 0$ ,  $St$  would be calculated using this equation:

$$St = AWC \times e^{-\left(\frac{APWL}{Sto}\right)} \quad (7)$$

(4) Change in soil moisture storage ( $\Delta St$ ) refers to the difference between the  $St$  values in this month and the previous month, as written below:

$$\Delta St = St - St_{i-1} \quad (8)$$

(5) Actual Evapotranspiration (EA) was determined based on P-PE:

- If  $P-PE > 0$ ,  $AE = PE$
- If  $P-PE < 0$ ,  $AE$  would be calculated using this equation:

$$AE = P + \Delta St \quad (9)$$

(6) Surplus and deficit refer to the difference between monthly precipitation and evapotranspiration. Surplus ( $S$ ) would be calculated if  $P > PE$ . In contrast, deficit ( $D$ ) would be estimated for months where  $P < PE$ . The equations used are as follows:

$$S = (P - PE) - \Delta St \quad (10)$$

If  $S$  is negative,  $S = 0$ .

$$D = PE - AE \quad (11)$$

If  $D$  is negative,  $D = 0$ .

**Drought Index Calculation**

The Palmer drought index considers three additional variables beyond water balance: Soil moisture replenishment (recharge), soil moisture depletion (loss), and runoff. It also factors in the depth of the soil layer that holds water (AWC) by dividing the soil into the top or surface layer and the bottom or underlying layer. The surface layer is assumed at a depth of 1 inch (approximately 25 mm) from the surface (Palmer, 1965) while the underlying layer is the remaining depth, calculated from 25 inches below the surface downwards to represent the depth of the root zone in the area.

The Palmer drought index comprises the Z index, PHDI, and PDSI. The Z index is a moisture anomaly index that pinpoints the

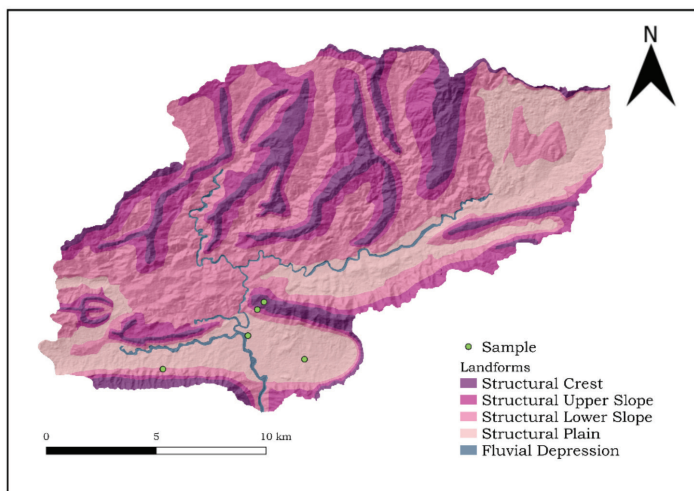


Figure 2: Map of the soil sampling locations

beginning and end of a wet or dry spell (Yan *et al.*, 2013). It is an empirical approach used to calculate the drought index for a known Z value that can be used to define the Palmer drought index using PHDI and PDSI. The main difference between the two indices is that PHDI describes an area's hydrological drought while PDSI refers to meteorological drought. The components used to compute the Z index, PHDI, and PDSI are explained below:

(1) Soil moisture in the surface and underlying layers with the capacity to store water is considered a drought factor as it controls water recharge and depletion in the soil. There are three assumptions in its calculation.

- Moisture loss begins in the surface layer. After the water in the surface layer is completely drained, the underlying surface will start losing moisture.
- Moisture recharge begins in the surface layer. Excess water, if any, will seep into the underlying layer after the surface layer is saturated.
- Runoff occurs only when both layers are saturated.

(2) The climatologically appropriate rainfall for existing conditions (CAFEC rainfall) was calculated using four climate parameters: Actual and potential monthly averages of evapotranspiration ( $\alpha$ ), moisture recharge ( $\beta$ ), runoff ( $\gamma$ ), and moisture loss ( $\delta$ ). These coefficients were defined as follows:

$$\alpha = \frac{\overline{EA}}{\overline{PE}} \tag{12}$$

$$\beta = \frac{\overline{R}}{\overline{PR}} \tag{13}$$

$$\gamma = \frac{\overline{RO}}{\overline{PRO}} \tag{14}$$

$$\delta = \frac{\overline{L}}{\overline{PL}} \tag{15}$$

(3) CAFEC precipitation was obtained by:

$$\hat{P} = \widehat{ET} + \hat{R} + \widehat{RO} - \hat{L} \tag{16}$$

where  $\widehat{ET}$ ,  $\hat{R}$ ,  $\widehat{RO}$ , and  $\hat{L}$ :

$$\widehat{ET} = \alpha \times PE \tag{17}$$

$$\hat{R} = \beta \times PR \tag{18}$$

$$\widehat{RO} = \gamma \times PRO \tag{19}$$

$$\hat{L} = \delta \times PL \tag{20}$$

(4) The moisture anomaly index (Z index) was defined as:

$$Z = d \times K \tag{21}$$

where the rainfall deficiency ( $d$ ) was:

$$d = P \times \hat{P} \tag{22}$$

and the standardisation constant  $K$  for climate characteristics was:

$$K = \frac{17.67}{\sum_{i=1}^2 \bar{D} \times K'} \times K' \tag{23}$$

$$K' = 1.5 \log_{10} \left( \frac{(\overline{EP} + \overline{R} + \overline{RO})}{\overline{P} + \overline{L}} + 2.8 \right) + 0.5 \tag{24}$$

$$\bar{D} = |\overline{d}| \tag{25}$$

(5) The PHDI and PDSI were calculated using the equations below:

$$X = X_{i-1} + \Delta X \tag{26}$$

where  $\Delta X$  was defined as:

$$\Delta X = \left( \frac{Z}{3} \right)_i + (-0.103 \times X_{i-1}) \tag{27}$$

for the first month,  $X_{i-1} = 0$ .

Table 3 shows the classification of the index and its respective code for a shorter naming purpose.

(6) Effective wetness ( $U_w$ ) and dryness ( $U_D$ ) were computed using the equations below:

$$U_w = Z + 0.15 \tag{28}$$

$$U_D = Z - 0.15 \tag{29}$$

(7) The amount of moisture required to end a wet or dry spell was calculated as follows:

$$Q = Ze + V - U \tag{30}$$

where  $Ze$  and  $V$  were defined as:

$$Ze = -2.691 \times X_{i-1} - 1.5 \tag{31}$$

$$V = \sum_{j=0}^{j=j^*} U_{i-j} \tag{32}$$

Table 3: Palmer Drought Index classification

Drought Index	Classification	Code
4.00 or more	Extremely wet	W5
3.00 to 3.99	Severely wet	W4
2.00 to 2.99	Moderately wet	W3
1.00 to 1.99	Slightly wet	W2
0.50 to 0.99	Incipient wet spell	W1
0.49 to -0.49	Near normal	N
-0.50 to -0.99	Incipient dry spell	D1
-1.00 to -1.99	Slightly dry	D2
-2.00 to -2.99	Moderately dry	D3
-3.00 to -3.99	Severely dry	D4
-4.00 or less	Extremely dry	D5

- (8) The probability ( $Pe$ ) of the ending of a wet or dry spell was calculated using the equation below:

$$Pe = \frac{v}{q} \times 100 \quad (33)$$

- (9) The PDSI was determined using the same assumption as the PHDI, although the calculation was categorised into three type to distinguish between wet and dry spells, as follows:

- X1: Drought index during the onset of a wet spell
- X2: Drought index during the onset of a dry spell
- XX3: Drought index during an established wet or dry spell

## Results and Discussion

Water plays a crucial role in meeting the needs of various sectors of human life. It is therefore necessary to understand the quantitative state of this vital natural resource, for instance, by calculating water availability. The Thornthwaite

equation for meteorological water balance yields not only estimates of water surplus or deficit, but also other supporting information such as Accumulated Potential Water Loss (APWL), soil moisture and its changes, and actual evapotranspiration. To obtain factors contributing to drought, data on rainfall, potential evapotranspiration, and soil moisture capacity should be first measured and analysed.

Three rain stations with known locations and data availability were used to analyse the rainfall data. One station was located within the upper Luk Ulo Watershed (Karangsambung Station) while two others were outside the watershed (Wadaslintang and Singomerto Stations). To spatialise the rainfall data (regional rainfall), each station's area of influence or proximal area was mapped using the Thiessen polygon method (Figure 3). This process was based on the principle that this area spans half the distance between one station and the nearest one. As a result, it produced three proximal zones designated as the Karangsambung, Wadaslintang, and Singomerto areas.

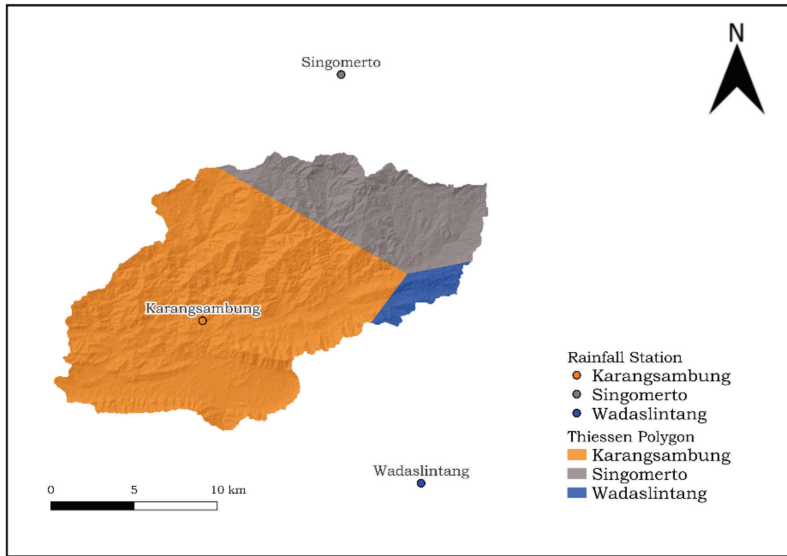


Figure 3: Thiessen polygons as units of analysis

As an approach to understanding the hydrological cycle of a watershed system, the water balance approach treats rainfall as the system’s input and potential evapotranspiration as the output. For this reason, water balance was calculated by first identifying months with higher or lower evapotranspiration (PE) than rainfall (P). Subtracting evapotranspiration from rainfall can produce a positive difference

( $P > PE$ ) or a negative difference ( $P < PE$ ). As seen in Figure 4, the 10-year P and PE averages showed positive differences from January to May and from October to December, defined as wet months or periods of potential surplus. Conversely, negative differences were observed from June to September, indicating dry months or periods of potential deficits (Nugroho *et al.*, 2019).

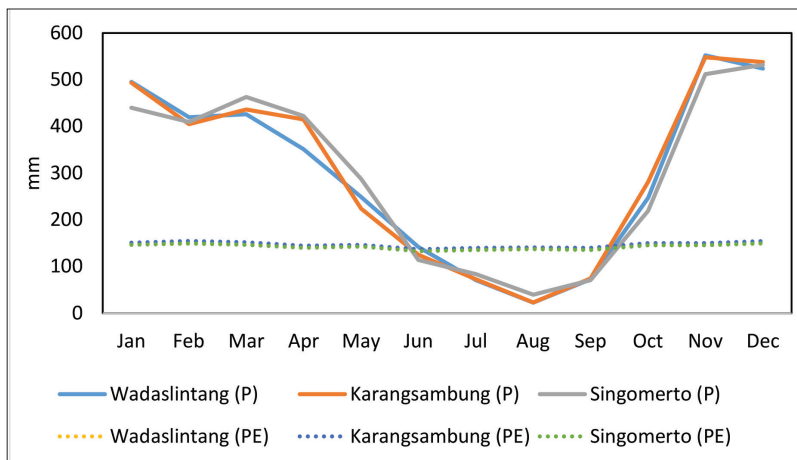


Figure 4: Average monthly Precipitation (P) and Potential Evapotranspiration (PE) in the proximal areas of Wadaslintang, Karangsambung, and Singomerto stations in the upper Luk Ulo Watershed (2011-2020)

Months in which potential evapotranspiration exceeded rainfall (negative difference) were used to determine Accumulated Potential Water Loss (APWL). The absolute value of the negative P-PE in one dry month was summed cumulatively with that of the following months. From 2011 to 2022, APWL peaked between August and November. APWL peaks represent the accumulation of APWL for that year. As shown in Figure 5, 2019 saw the highest potential losses of 744.64 mm and 720.55 mm in the Wadaslintang and Karangsembung areas, respectively.

Meanwhile, 2015 was the year with the highest potential loss, amounting to 667.31 mm, in the Singomerto area. In 2016, there was no potential water loss at the three stations as they showed positive P-PE differences. This can be attributed to the La Nina event, which brought high rainfall that year. Lestari *et al.* (2019) found that the 2016 La Nina increased rainfall to above its normal average starting in the boreal summer, i.e., June. Similarly, the rainfall in June 2016 at the three stations was higher than that of the same month in other years. The elevated rainfall lasted until the end of the year, although a slight decrease was observed in August, a month typically associated with peak dryness.

Soil moisture or Available Water Capacity (AWC) was determined by overlapping soil

texture with land use data and calculating the weighted average for each polygon. Figure 6 (a) shows the soil texture map derived from the obtained soil samples while Figure 6 (b) shows the land use map. Soil texture determines the soil’s availability to retain moisture, whereas land use serves as a proxy of the plant root zone. The AWC obtained was assumed to remain constant from 2011 to 2020 at 131.81 mm (Wadaslintang Station), 130.7 mm (Karangsembung Station), and 130.09 mm (Singomerto Station).

AWC was used to measure monthly soil moisture using APWL. In months where APWL equalled 0, their soil moisture was assumed to be equal to the AWC, suggesting no potential water loss and water-saturated soil conditions. Conversely, in months with  $APWL > 0$ , their soil moisture is lower than the AWC. This indicates potential water loss, where the available water could not saturate the soil. As shown in Figure 7, from January to April, the monthly average of soil moisture in the Wadaslintang and Karangsembung areas met the AWC. In contrast, the Singomerto area maintained saturated soil moisture until May, with only a minor decline in February. Soil moisture continued to decrease until the lowest value in August at approximately 30 mm. Then, from September to November, the soil moisture was replenished and began to saturate until December.

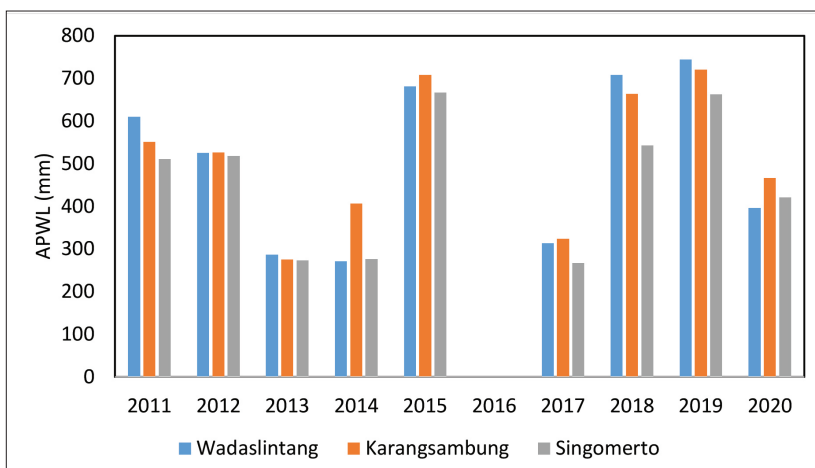


Figure 5: Total annual APWL (2011-2020)

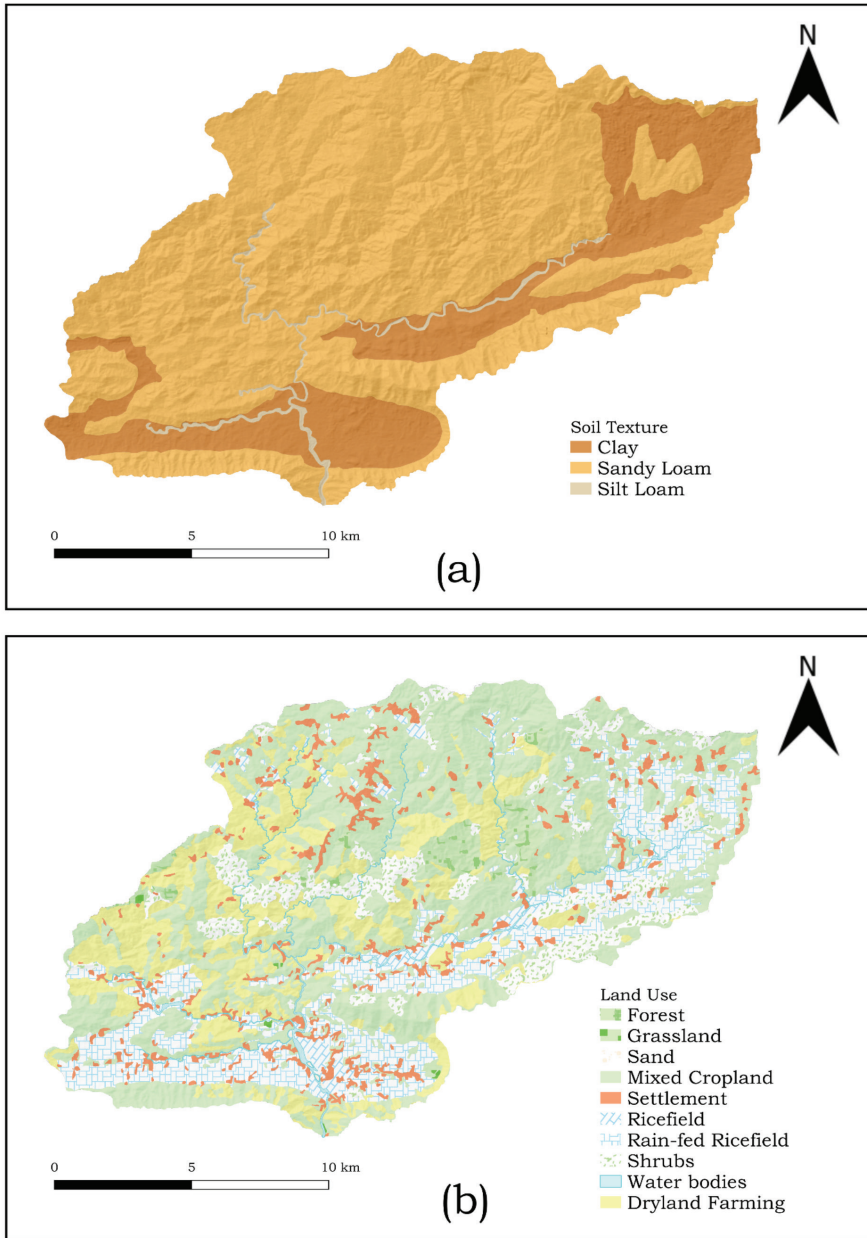


Figure 6: Map of (a) the soil texture and (b) land use

Actual evapotranspiration (AE) shows the amount of evapotranspiration that corresponds to actual water availability. In contrast, potential evapotranspiration (PE) is estimated based on the assumption that the watershed is saturated. Therefore, AE is calculated from

the difference between rainfall and potential evapotranspiration. A positive difference indicates that the available water equals or exceeds potential evapotranspiration; in this case, the actual and potential values are equal. On the contrary, a negative difference means

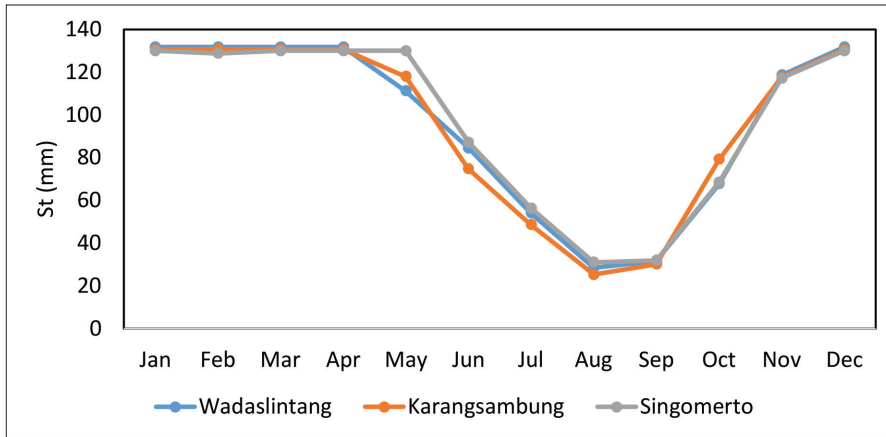


Figure 7: Monthly averages of soil moisture (St) (2011-2020)

the available water is lower than the potential evapotranspiration. Thus, rainfall and existing soil moisture supply the water used in potential evapotranspiration. The latter is indicated by a negative change in soil moisture.

The AE trend showed that from January to April, the monthly means in the Wadaslintang and Karangsembung areas were similar to their average PE. In the Singomerto area, this occurred from January to May. AE then declined until its lowest point in August (Wadaslintang and Karangsembung) and September (Singomerto) before increasing and approaching PE in November. At this point, AE was equal to PE+1 mm in the Wadaslintang and Karangsembung

areas while AE was the same as PE in the Singomerto area. December was the third month that the three proximal areas showed similar mean values in their AE and PE. This trend was visually identical to soil moisture, including the lowest means in the driest month, August. This suggests that soil moisture correlates and even contributes to evapotranspiration.

Accumulated water availability in the three proximal areas of the rain gauge stations in the upper Luk Ulo watershed showed a fluctuating trend throughout the observation period (Figure 8). The three areas saw the highest water availability in 2016; 4,166 mm in Wadaslintang, 4,316 mm in Karangsembung, and 3,725 mm in

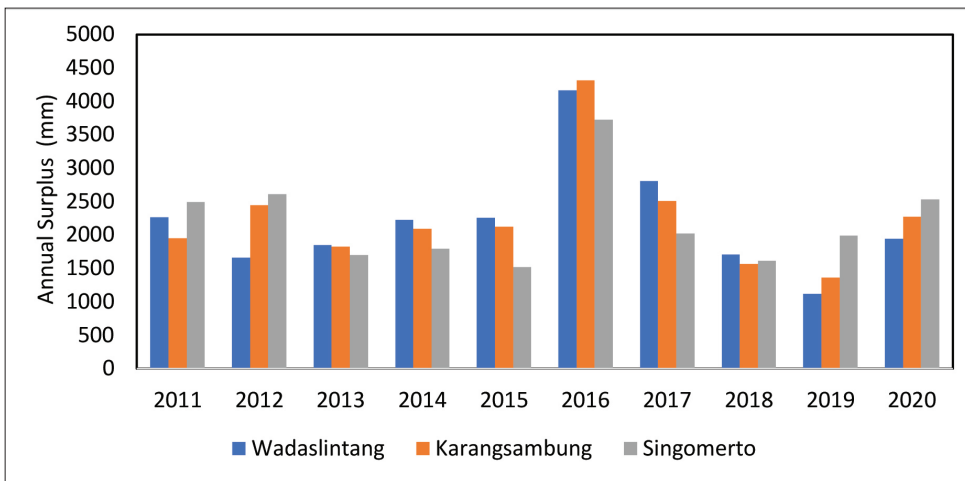


Figure 8: Water availability showing annual surplus (2011-2020)

Table 4: Annual water availability (in mm) of the upper Luk Ulo Watershed (2011-2020)

Region/Year	2011	2012	2013	2014	2015	2016	2017	2018	2019	2020
Wadaslintang	2,269	1,661	1,848	2,226	2,259	4,166	2,804	1,715	1,120	1,946
Karangsambung	1,947	2,445	1,826	2,091	2,125	4,316	2,509	1,565	1,362	2,272
Singomerto	2,495	2,610	1,703	1,793	1,519	3,725	2,026	1,610	1,985	2,533

Singomerto (Table 4). Meanwhile, the lowest water availability was identified in 2019 for Wadaslintang and Karangsambung (1,120 mm and 1,362 mm) and in 2015 for Singomerto (1,519 mm). Differences in trends in water availability were identified in 2012 and 2019. In 2012, Wadaslintang and Singomerto showed an increasing trend while Karangsambung indicated a decreasing water availability. Then, in 2019, low availability was detected in Wadaslintang and Karangsambung, but the opposite was observed in Singomerto. These differences likely reflect local variations in rainfall patterns.

Figure 9 (a-d) presents the monthly CAFEC coefficients ( $\alpha$ ,  $\beta$ ,  $\gamma$ ,  $\delta$ ) for the three proximal areas during the observation period. From January to

April, the coefficient  $\alpha = 1$ , indicating that the monthly average of AE matched PE. From May to October, this coefficient was smaller than 1, indicating  $AE < PE$  or that the water availability was insufficient to meet potential demand. This interpretation also applies to the other CAFEC coefficients.

The  $\beta$  coefficient indicated no actual and potential soil moisture recharge from January to May due to water-saturated soil. As division by zero yields an undefined value,  $\beta$  was assigned a value of 1 in these months, assuming actual recharge fulfilled the potential. In June, the Karangsambung area showed  $\beta = 0$ , meaning that the mean actual Recharge (R) was 0 and could not meet the positive Potential Recharge (PR).

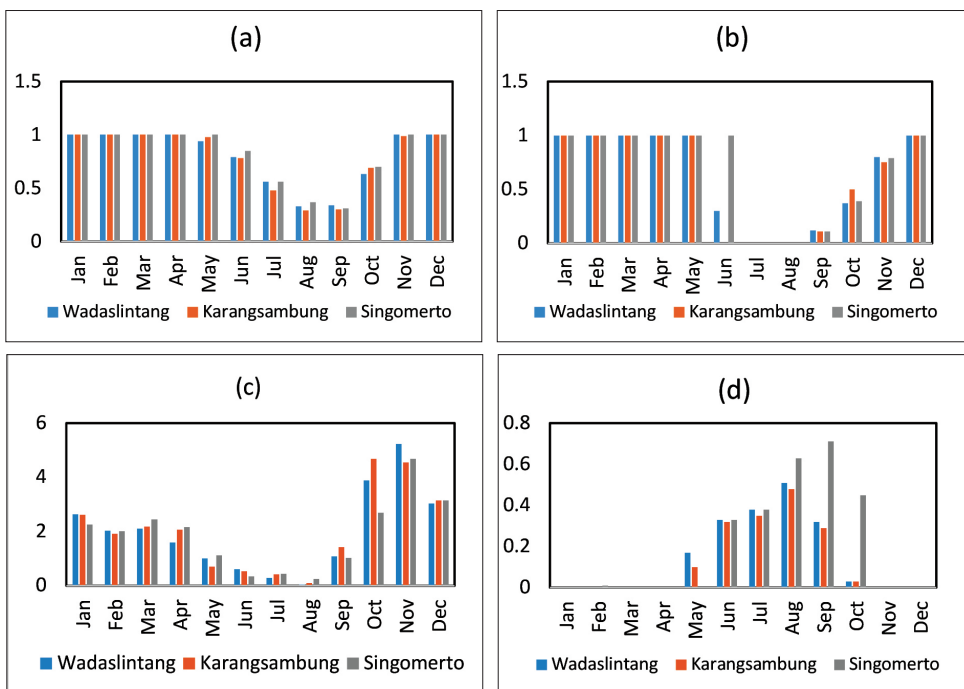


Figure 9: CAFEC coefficients: (a)  $\alpha$ , (b)  $\beta$ , (c)  $\gamma$ , and (d)  $\delta$

The coefficient  $\gamma$  was generally higher than 1 from January to April and from September to December, suggesting actual runoff (RO) was higher than the potential value (PRO). Meanwhile,  $\delta$  remained constant at 0 from January to April and from November to December, but dropped below 1 during other months. The latter indicated actual moisture loss (L) that was higher than the potential value (PL). Notably, from August to November,  $\delta$  had a high value in Singomerto, a different trend from other stations. This suggests that the actual moisture loss in these months was higher in Singomerto, making it closer to the potential value.

The four coefficients represent the climatically appropriate values for existing conditions (CAFEC) in the watershed from 2011 to 2020. The multiplication product between these coefficients and their respective potential values illustrates normal and basic conditions in the CAFEC rainfall calculation. Unlike the four coefficients that had similar monthly values throughout the 10 years of observation, the CAFEC value would be unique for each month of each year, thus, providing normal conditions that are distinctive at each time rather than a generalised average.

Figure 10 shows the annual average Z Index in the proximal zones of the three rain stations. In 2016, positive index values were detected in all areas: 1.89 in Wadaslintang, 1.93 in Karangsembung, and 1.62 in Singomerto,

indicating wet conditions throughout the year. The lowest index was found in 2012 in Wadaslintang (-0.94), 2011 in Karangsembung (-0.55), and 2015 in Singomerto (-0.66). The Z index multiplies rainfall deficiency by a predetermined weight according to the climate characteristics of each rain station to facilitate quick comparison. Here, rainfall deficiency provides a reference for identifying unique trends in dry or wet months. The other two Palmer drought indices, PHDI and PDSI were computed based on the Z index while considering conditions in the previous month. This way, the drought indices will create cumulative correlations between one another.

Figure 11 shows the number of wet or dry spells categorised into W1-W5, N, or D1-D5 according to PHDI values (Table 2). Slightly dry spells (D2) were dominant in the Wadaslintang and Karangsembung areas (n = 35 months). Meanwhile, the Singomerto area mainly saw near-normal conditions (N) (n = 48 months). In Wadaslintang, incipient dry spells occurred most frequently in the 2012–2014 and 2019–2020 periods. In Karangsembung, the high frequency of incipient dry spells was found in 2012 and from 2018 to 2020. On the other hand, Singomerto experienced more near-normal conditions from 2011 to 2013 and 2020. Besides D2 and N, incipient dry spells (D1) had the third-highest frequency, with 24 occurrences in Singomerto.

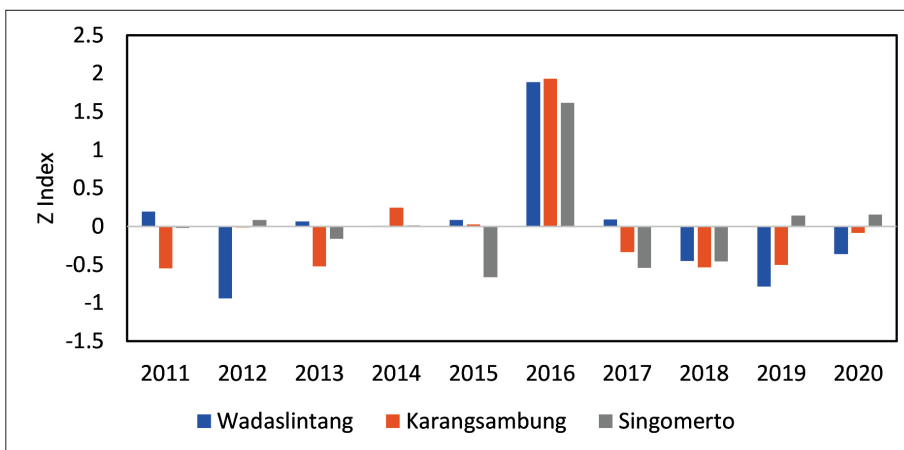


Figure 10: Annual averages of the Z index (2011-2020)

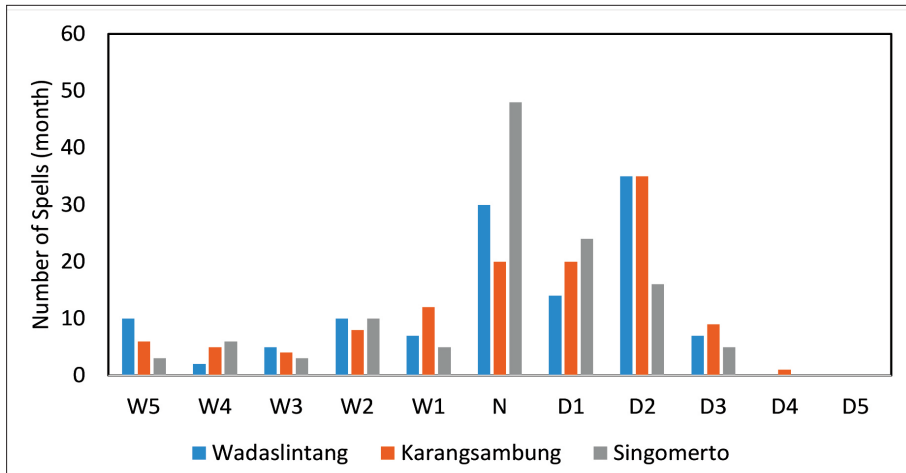


Figure 11: Number of wet or dry spells according to PHDI in the three proximal areas (2011-2020)

Figure 12 displays maps of the annual average PHDI and the distribution of near-normal, dry, or wet spells in the upper Luk Ulo Watershed, depicted with the proximal areas of the three rain stations. The upper watershed showed incipient dry spells and near-normal conditions in 2011, which then turned into widespread incipient dry spells in 2012 and near-normal in 2013. The following year, 2014, incipient dry spells were observed in the Karangsembung and Singomerto areas, as well as in the Wadaslintang area, which marked the most severe and extensive drought in the 2011–2020 period, affecting an area of 257.38 km<sup>2</sup>. In 2015, the index shifted towards wetter conditions: the driest months in Singomerto and Wadaslintang returned to near-normal levels while Karangsembung experienced incipient wet spells.

The year 2016 was the wettest at all three stations, covering an area of 202.14 km<sup>2</sup>. These results corresponded to the year-round water surplus or high water availability caused by

above-average rainfall. The rain deficiency in the middle of 2016 was positive and unusually high, despite the period normally being characterised by low rainfall or dry months. Then, in 2017, the extremely wet conditions subsided to incipient wet spells were dominant.

In 2018, the upper watershed began to experience incipient dry spells in Karangsembung and Singomerto. That year was the driest in Singomerto, with a PHDI of -1.44 (Table 5). Near-normal conditions prevailed in the Wadaslintang area from 2018 to 2019 and then turned into incipient dry spells in 2020. In 2019, Wadaslintang recorded its driest year (PHDI = -1.31). As in 2012, Singomerto experienced near-normal conditions in 2019, while other areas saw dry to incipient dry spells. During the research period, Singomerto had extremely wet spells in 2016 and 2019 a different trend from other areas. This is likely due to various topographic factors that allow for variations in rainfall and consequently, drought occurrences.

Table 5: Annual average PHDI of the upper Luk Ulo Watershed (2011-2020)

Region/Year	2011	2012	2013	2014	2015	2016	2017	2018	2019	2020
Wadaslintang	0.41	-1.32	-0.55	-0.96	-0.29	3.38	2.90	-0.07	-1.31	-1.50
Karangsambung	-0.72	-1.11	-0.33	-1.51	0.74	3.58	1.94	-0.98	-1.10	-1.15
Singomerto	-0.05	0.04	-0.10	-1.04	-0.42	1.82	1.80	-1.44	-0.15	-0.14

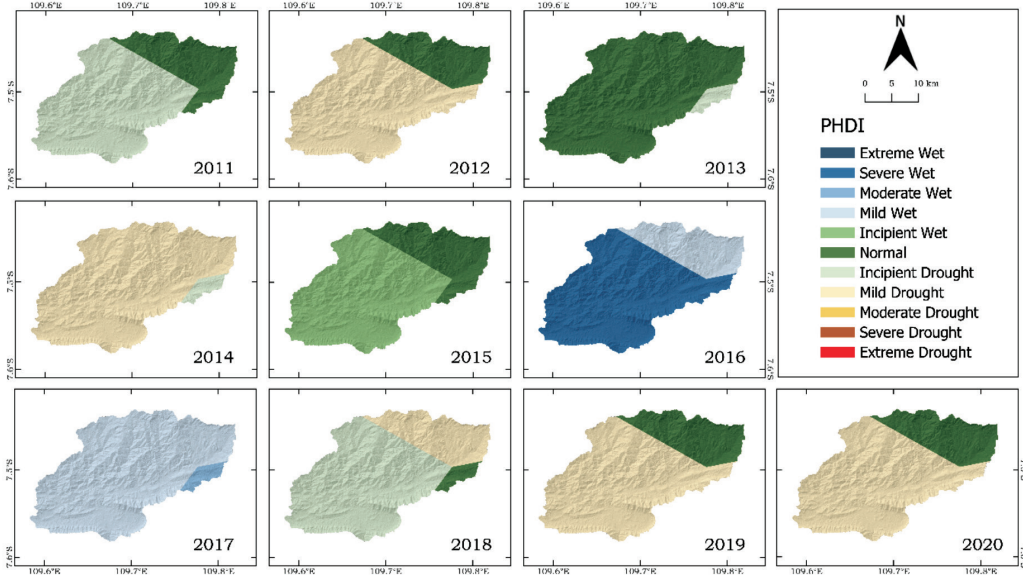


Figure 12: PHDI maps of the upper Luk Ulo Watershed (2011-2020)

Figure 13 shows the number of wet or dry spells according to PDSI values. In Singomerto, the near-normal condition remains dominant throughout the research period, as seen with PHDI. However, the resulting near-normal classifications differed: 48 near-normal occurrences in PHDI and 28 in PDSI. The same results were found in Wadaslintang and Karangsembung: 30 and 20 occurrences in PHDI, but 13 and 4 in PDSI, respectively. Conversely,

more spells were categorised as incipient dry spells. Such a significant difference resulted in widespread, incipient dry spells in the upper watershed, where Wadaslintang experienced 57 dry months, Karangsembung experienced 69 dry months, and Singomerto experienced 47 dry months. Furthermore, more spells were classified as wet and dry spells, except for those categorised initially as D1 in PHDI. These indicated a transition to more severe dry periods.

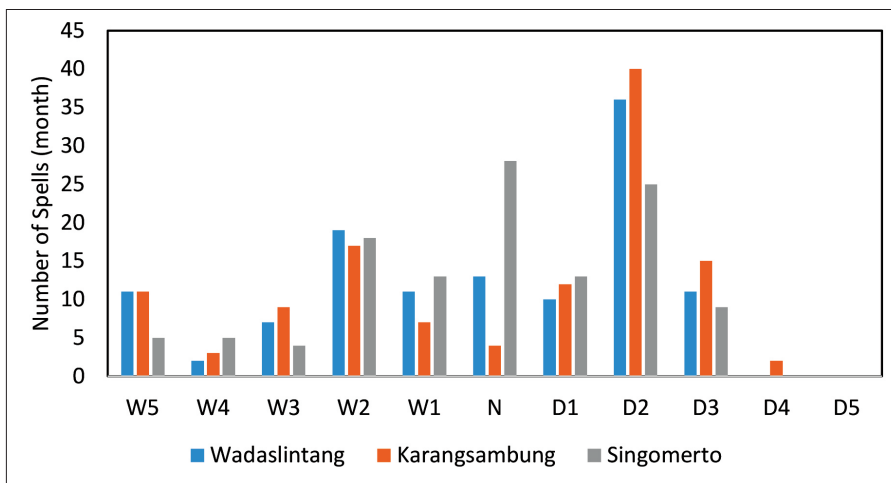


Figure 13: Number of wet or dry spells according to PDSI in the three proximal areas (2011-2020)

Nevertheless, while no extreme dry spells were found in the three proximal areas, there were three severe dry spells, according to PDSI, compared with only one dry spell in the PHDI classification. Also, there were significantly more events classified as wet spells but less as near-normal by PDSI.

Transitions towards more severely dry or wet months are closely related to determining the end and beginning of a spell in the PDSI calculation, which is based on probability. A spell does not necessarily end with a normal or opposite index value, but instead based on a 100% probability obtained by comparing the accumulated moisture and humidity required to end a spell. In this case, PDSI appeared to be more sensitive to drought indicators, as it produced a drier and further-from-normal index. Weber and Nkemdirim (1998) stated that PDSI can detect the beginning and end of a spell more quickly, up to three months earlier than PHDI. However, both indices can describe a unique phenomenon at any time such as the extreme wet spells in 2016 and severe dry spells in 2014. These outcomes reflect their differing concepts and applications: PHDI for hydrological drought, and PDSI for meteorological drought.

In addition, since both PDSI and PHDI are derived from the same parameter, i.e., the Z index, their calculations likely produce similar values. However, identifying the beginning and end of a spell can result in different values between the two. As such, differences can usually be detected at the beginning and end of a dry or wet spell, e.g., earlier increase in the degree of severity or earlier return to near-normal condition. Figure 14 maps the number of spells categorised according to PDSI. The classification results in the 2011-2018 period differing from PHDI. For instance, in 2011, PDSI

classified the upper watershed as experiencing a near-normal condition, but PHDI calculations yielded incipient dry spells in Karangsambung.

A shift towards more severely wet months was observed in 2016, as evidenced by a difference by one degree between the PHDI and PDSI classifications: From incipient to moderately wet in Singomerto (PDSI = 2.22) and from severe to extremely wet in Wadaslintang (4.08) and Karangsambung (4.84) (Table 6). These might be caused by prolonged high rainfall that led to a low probability of the ending of the wet spell. As a result, even though a one-degree decline was observed in 2017, the PSDI values were consistently above 1.

PDSI generally indicated that the 2014 drought had weakened and was trending towards near-normal conditions in the following years. In comparison, PHDI classified most of the upper Luk Ulo watershed as having incipient dry spells. PDSI classified Singomerto as having incipient dry spells in 2014 and then incipient dry spells in 2015. This weakening drought intensity was also observable from the number of near-normal months that became wetter, especially in Singomerto. In addition, the annual average showed a shift from incipient dry spells to near-normal conditions. The year 2014 was the driest for Karangsambung, which was similar to the PHDI classification results. PDSI showed prevailing incipient dry spells in 2018 (similar to 2014), which was distributed more widely than the PHDI classification. The year 2018 was the driest for Singomerto, according to both indices.

The annual average of drought events in 2019 and 2020 showed similar classifications between PDSI and PHDI, i.e., prevailing incipient dry spells in the upper watershed,

Table 6: Annual average PDSI of the upper Luk Ulo Watershed (2011-2020)

Region/Year	2011	2012	2013	2014	2015	2016	2017	2018	2019	2020
Wadaslintang	0.35	-1.48	-0.25	-0.74	0.15	4.08	3.08	-0.68	-1.31	-1.14
Karangsambung	-0.44	-0.70	-0.22	-1.44	0.91	4.84	2.06	-1.33	-1.00	-1.25
Singomerto	0.02	-0.03	0.13	-0.55	-0.49	2.22	1.71	-0.95	0.01	-0.18

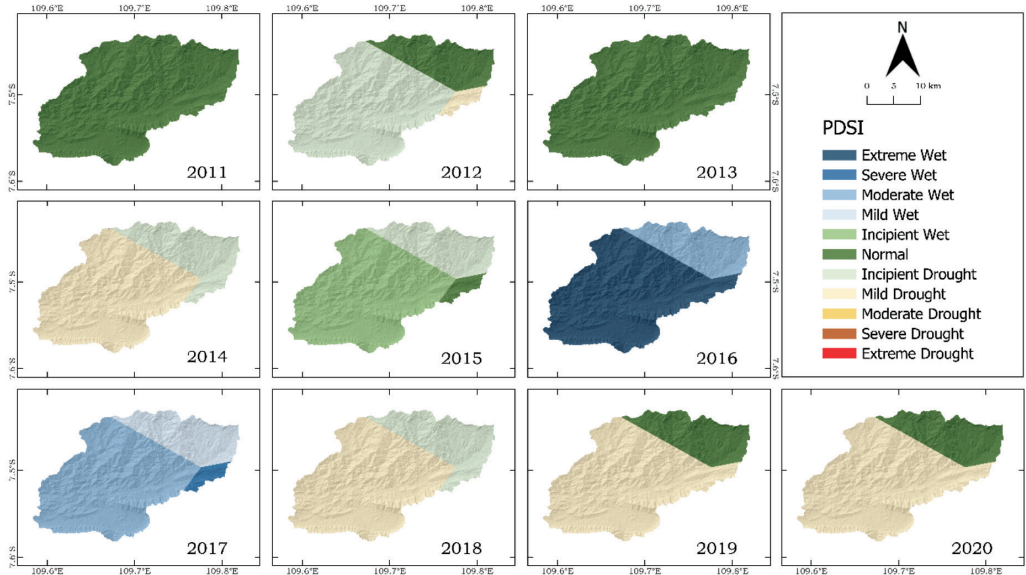


Figure 14: PDSI maps of the upper Luk Ulo Watershed (2011-2020)

especially the Wadaslintang and Karangsembung areas. As a result, 2019 and 2020 were the years with the most severe and extensive drought, affecting 202.14 km<sup>2</sup>. As for Singomerto, both indices showed near-normal conditions. Similar classification results between PDSI and PHDI were also in line with the insignificant difference in the duration of the identified spells. Singomerto experienced near-normal conditions while the proximal areas of the other two stations showed incipient dry spells. These results corresponded to water availability in both years. In 2019, water availability increased significantly from the previous year in Singomerto, but decreased in Wadaslintang and Karangsembung. Both PHDI and PDSI categorised 2019 as the driest year in Wadaslintang.

The analysis of water availability in the upper Luk Ulo Watershed from 2011 to 2020 reveals fluctuations spatially and temporally. These were mainly influenced by fluctuations in rainfall and evapotranspiration. The year 2016 was the wettest, with all three regions recording the highest water availability, as well as PHDI and PDSI values indicating severe and extremely wet period, respectively. The wet conditions impacted an area of 257.38 km<sup>2</sup>,

showing a hydrological response that affects an extensive and majority part of the research area. This condition can affect an area in two ways: It signals abundant water resources for agricultural and domestic needs, but extreme wet conditions may also lead to catastrophic flooding. This is consistent with the rain-fed rice fields that dominate the region’s agricultural landscape. The strong dependence on meteorological water availability may lead to higher runoff as the region lacks irrigation infrastructure (Hadi *et al.*, 2020), as well as greater agricultural drought propagation (Rasjiddin *et al.*, 2020).

Conversely, several years within this period were marked by low availability of water and droughts. The lowest water availability occurred in 2019 in Wadaslintang and Karangsembung and in 2015 in Singomerto. However, droughts were identified in different years, which were 2019 in Wadaslintang, 2014 in Karangsembung, and 2018 in Singomerto. The discrepancy between water availability and drought spells is thought to be due to differences in approach between the two calculations, considering that the Palmer drought indices approach soil moisture conditions differently, and they are influenced by the conditions of prior months,

meaning drought classifications may not always align with observed water availability.

The upper Luk Ulo Watershed's vulnerability to drought condition is reflected through the higher number of dry spells than the wet spells. This condition highlights the urgency of adaptive mitigation strategies to address extreme climatic conditions in the region, as climate change exacerbates hydrometeorological disasters into a more catastrophic level. Mitigation efforts might involve the enhancement of water storage facilities to handle excessive water during wet spells, as well as keeping enough water availability during dry spells. High agricultural activities in the region also requires significant adaptation measures. Switching to highly tolerant crops and changing the type of crops for each season are examples of what local farmers in the area have done (Sekaranom *et al.*, 2021). Collaboration within relevant governmental agencies and local communities is essential such as implementing effective information channel as an early warning system and adjustments to planting calendars, allowing for better planning in response to extreme weather events.

## Conclusions

This study presents a quantitative assessment of water availability and drought conditions in the upper Luk Ulo Watershed from 2011 to 2020. Water availability was the highest in 2016 (4,166 mm in Wadaslintang, 4,316 mm in Karangsambung, and 3,725 mm in Singomerto), the lowest in 2019 (1,120 mm in Wadaslintang and 1,364 mm in Karangsambung) and 2015 (1,523 mm in Singomerto). These variations were closely associated with fluctuations in with rainfall and evapotranspiration.

Both PHDI and PDSI identified 2016 as the year with the most severe and extensive wet spells in Wadaslintang and Karangsambung (severely wet conditions according to PHDI and extremely wet conditions according PDSI), affecting an area of 257.38 km<sup>2</sup>. In 2016, the PHDI values were 3.38 in Wadaslintang, 3.58 in

Karangsambung, and 1.82 in Singomerto. The PDSI values were 4.08 in Wadaslintang, 4.84 in Karangsambung, and 2.22 in Singomerto. According to PHDI, the driest years were 2019 in Wadaslintang (-1.31), 2014 in Karangsambung (-1.51), and 2018 in Singomerto (-1.44).

The driest year according to PDSI were the same for each station (-1.31 in Wadaslintang, -1.44 in Karangsambung, and -0.95 in Singomerto). PHDI classified 2014 as the year with the most severe and widespread drought, as evident in the prevailing incipient dry spells in the Karangsambung and Singomerto areas (around 257.38 km<sup>2</sup>). Meanwhile, PDSI classified 2019 and 2020 as the years with prevailing incipient dry spells in Karangsambung and Wadaslintang (202.14 km<sup>2</sup>). Based on the number of spells, both indices showed that the upper Luk Ulo Watershed mainly saw more dry than wet spells. This reflects the region's proneness to extreme hydrometeorological conditions, especially drought and occasional flooding. Extensive rain-fed rice fields that depends on rainfall may require irrigational intervention, thus, ensuring sustainable food production in the region.

## Acknowledgements

This research was funded by Universitas Gadjah Mada, Indonesia through the Final Project Recognition Grant Number 5075/UN1.P.II/Dit-Lit/PT.01.01/2023. The authors would like to thank the reviewers for their valuable input and contribution in improving the quality of this article.

## Conflict of Interest Statement

The authors declare that they have no conflict of interest.

## References

- American Meteorological Society. (2019). *Drought - Glossary of Meteorology*. Ametsoc.org. <https://glossary.ametsoc.org/wiki/Drought>

- Arsal, T., Sumartono, Basri & Anam, M. (2018). Effect of sand mining on social-economic and ecology of communities in Lukulo River areas Kebumen Central Java. *Komunitas*, 10(2), 270-278.
- Aryo, B., & Lubis, R. H. (2014). *Kebencanaan dan kesejahteraan: Konsep dan praktek*. Depok: Lembaga Kemitraan Pembangunan Sosial (LKPS).
- Asriningrum, W., Harsanugraha, W. K., & Prasasti, I. (2019). *Bunga rampai pemanfaatan data penginderaan jauh untuk mitigasi bencana banjir*. Bogor: PT Penerbit IPB Press.
- Barry, R. G. (2021). *The world hydrological cycle*. In *Water, earth, and man: A synthesis of hydrology, geomorphology, and socio-economic geography*. Taylor & Francis.
- Cheval, S. (2015). The standardised precipitation index—An overview. *Romanian Journal of Meteorology*, 12(1-2), 17-64.
- Dai, A., & NCAR. (2023). *The Climate Data Guide: Palmer Drought Severity Index (PDSI)*. <https://climatedataguide.ucar.edu/climate-data/palmer-drought-severity-index-pdsi>
- Dalezios, N. R., Gobin, A., Tarquis, A. M., & Eslamian, S. (2017). Agricultural drought indices: Combining crop, climate, and soil factors. *Handbook of Drought and Water Scarcity: Principles of Drought and Water Scarcity*.
- Dey, R., & Lewis, S. C. (2021). Chapter 6 – Natural disasters linked to climate change. In *The impacts of climate change* (pp. 177-193). Elsevier.
- Eslamian, S., Ostad-Ali-Askari, K., Singh, V. P., Dalezios, N. R., Ghane, M., Yihdego, Y., & Matouq, M. (2017). A review of drought indices. *International Journal of Constructive Research in Civil Engineering*, 3(4).
- Faiz, M. A., Liu, D., Fu, Q., Naz, F., Hristova, N., Li, T., Niaz, M. A., & Khan, Y. N. (2020). Assessment of dryness conditions according to transitional ecosystem patterns in an extremely cold region of China. *Journal of Cleaner Production*, 255, 120348.
- Faiz, M. A., Zhang, Y., Zhang, X., Ma, N., Aryal, S. K., Ha, T. T. V., Baig, F., & Naz, F. (2022). A composite drought index developed for detecting large-scale drought characteristics. *Journal of Hydrology*, 605, 127308.
- Funk, C., & Shukla, S. (2020). *Drought early warning and forecasting: Theory and practice*. Elsevier Science.
- Gao, H., Tang, Q., Ferguson, C. R., Wood, E. F., & Lettenmaier, D. P. (2010). Estimating the water budget of major US river basins via remote sensing. *International Journal of Remote Sensing*, 31(14), 3955-3978.
- Government of the Kebumen Regency. (2015). *Drought in Kebumen Widespread*. kebumen.kab.go.id. [https://www.kebumenkab.go.id/index.php/web/news\\_detail/7/3758](https://www.kebumenkab.go.id/index.php/web/news_detail/7/3758)
- Hadi, M. P., Syamsiyyah, N. J. L., & Annisa, L. (2020). Unit hydrograph method for curve number validation in hydrological modelling: Case study of Welaran Watershed, Karangsambung, Kebumen. In *IOP Conference Series: Earth and Environmental Science* (Vol. 451, No. 1, p. 012077). IOP Publishing.
- Hidayati, I. N., & Suryanto, S. (2015). Climate change impact on agricultural production and adaptation strategies on drought-prone areas. *Jurnal Ekonomi & Studi Pembangunan*, 16(1), 42-52.
- Karl, T., Quinlan, F., & Ezell, D.S. (1987). Drought termination and amelioration: Its climatological probability. *Journal of Applied Meteorology and Climatology*, 26(9), 1198-1209.
- Kurniawan, A. R., Bisri, M., & Suhartanto, E. (2020). Drought analysis in Bedadung Watershed based on a Geographical Information System. *IOP Conference Series: Earth and Environmental Science* (Vol. 437, No. 1, p. 012024). IOP Publishing.

- Lee, S., Moriasi, D. N., Mehr, A. D., & Mirchi, A. (2024). Sensitivity of Standardised Precipitation and Evapotranspiration Index (SPEI) to the choice of SPEI probability distribution and evapotranspiration method. *Journal of Hydrology: Regional Studies*, 53, 101761.
- Lestari, D. O., Sutriyono, E., Kadir, S., & Iskandar, I. (2019). Impact of 2016 weak La Niña Modoki event over the Indonesian region. *GEOMATE Journal*, 17(61), 156-162.
- Liu, S., Shi, H., & Sivakumar, B. (2020). Socioeconomic drought under growing population and changing climate: A new index considering the resilience of a regional water resources system. *Journal of Geophysical Research: Atmospheres*, 125(15), e2020JD033005.
- Mediani, A., Fajar, M., Basuki, A., & Finesa, Y. (2019). Water balance and water requirements of rice plants for food security in mitigating drought disasters in the Samin sub-watershed. *Prosiding Seminar Nasional Geografi UMS X 2019*.
- Nugroho, A. R., Tamagawa, I., Riandraswari, A., & Febrianti, T. (2019). Thornthwaite-Mather water balance analysis in Tambakbayan watershed, Yogyakarta, Indonesia. *MATEC Web of Conferences* (Vol. 280, p. 05007). EDP Sciences.
- Palmer, W. C. (1965). *Meteorological drought* (Vol. 30). US Department of Commerce, Weather Bureau.
- Raharjo, P. D. (2009). Remote sensing and GIS data applications for monitoring degradation in the Upper Luk Ulo Watershed, Central Java. *Jurnal Manusia dan Lingkungan*, 17(1), 37-45.
- Rasjiddin, A. I., Sobirin, S., & Waryono, T. (2020). The potential of agricultural drought according to brightness and wetness index on Kebumen district. In *IOP Conference Series: Earth and Environmental Science* (Vol. 481, No. 1, p. 012060). IOP Publishing.
- Saifudin, S., & Raharjo, P.D. (2008). Measuring deposition rates to determine tolerance for sand and stone mining (Case study in the Upper Lukulo Watershed, Central Java). *Majalah Geografi Indonesia*, 22(1), 52-60.
- Sanim, B. (2018). *Sumber daya air dan kesejahteraan publik: Suatu tinjauan teoritis dan kajian praktis*. Bogor: IPB Press.
- Saputro, S. P., & Mulyasari, R. (2019). Aspect and criteria of geological conditions for groundwater quantity control. *Ilmu Teknik dan Kajian Multidisiplin dalam Mitigasi Bencana Nasional*, 1, 1-10.
- Sekaranom, A. B., Nurjani, E., & Nucifera, F. (2021). Agricultural climate change adaptation in Kebumen, central Java, Indonesia. *Sustainability*, 13(13), 7069.
- Sen, Z. (2015). *Applied drought modeling, prediction, and mitigation*. Elsevier Science.
- Shaw, R., Nguyen, H., Habiba, U., & Takeuchi, Y. (2011). Overview and characteristics of Asian Monsoon drought. In Shaw, R., & Nguyen, H. (Eds.), *Droughts in Asian Monsoon Region*. Emerald.
- Tefera, A. S., Ayoade, J. O., & Bello, N. J. (2019). Comparative analyses of SPI and SPEI as drought assessment tools in Tigray Region, Northern Ethiopia. *SN Applied Sciences*, 1, 1-14.
- Thompson, S. A. (2017). *Hydrology for water management*. Boca Raton: CRC Press.
- UN Office for the Coordination of Humanitarian Affairs (OCHA). (2011). *OCHA and Slow-onset Emergencies*. UN Office for the Coordination of Humanitarian Affairs (OCHA).
- Weber, L., & Nkemdirim, L. (1998). Palmer's drought indices revisited. *Geografiska Annaler: Series A, Physical Geography*, 80(2), 153-172.
- World Meteorological Organisation (WMO) and Global Water Partnership (GWP). (2016). *Handbook of Drought Indicators and*

- Indices. Integrated Drought Management Programme (IDMP), Integrated Drought Management Tools and Guidelines Series 2.* World Meteorological Organisation (WMO) dan Global Water Partnership (GWP).
- Yan, D., Shi, X., Yang, Z., Li, Y., Zhao, K., & Yuan, Y. (2013). Modified Palmer Drought Severity Index based on distributed hydrological simulation. *Mathematical Problems in Engineering*.